Elliptic Flow in Uranium-Uranium Collisions at $\sqrt{s_{\mathrm{NN}}} = 193$ GeV

Tom Callister
Carleton College

Department of Physics and Astronomy, University of California, Los Angeles
2012 Summer REU Program

September 9, 2012

Abstract

The hot, dense nuclear medium created in Gold-Gold collisions at RHIC exhibits strong, anisotropic collective motion, characterized by the elliptic flow coefficient v_2. v_2 has been extensively studied, and is thought to be related to the initial eccentricity ϵ of the colliding system and its resulting density, quantified by $\frac{1}{S}\frac{dN}{d\eta}$. Recently, RHIC has begun colliding Uranium ions. Collisions of these heavier, deformed uranium nuclei will introduce greater eccentricities, and were expected to increase the achievable value of $\frac{1}{S}\frac{dN}{d\eta}$ by 13%. Simulations therefore predict that central Uranium-Uranium collisions will yield a significant increase in v_2 over central Gold-Gold collisions. In this paper we present the first v_2 measurements from these Uranium-Uranium collisions. We find that Uranium collisions increase v_2 and $\frac{1}{S}\frac{dN}{d\eta}$, as expected. Contrary to predictions, however, we also find that v_2/ϵ vs. $\frac{1}{S}\frac{dN}{d\eta}$ deviates significantly from the universal curve set by Gold-Gold collisions.

1 Introduction

The majority of visible matter is made of up quarks, fundamental particles which interact via the strong force. Counterintuitively, as the separation between two quarks increases, so does the force between them. Any attempt to separate these particles will simply result in the creation of additional quarks to fill the resulting gap. For this reason, all quarks in nature are confined, bound in the form of hadrons. Quantum chromodynamics (QCD), however, predicts that beyond a cutoff temperature of 170 MeV [1], quarks actually become deconfined – past this point hadrons "melt" into their constituent quarks and gluons. The resulting state of matter is known as a quark-gluon plasma (QGP), as it very closely mirrors the freely-flowing positive and negative charges found in a conventional plasma. During the first 10^{-4} s after the Big Bang, our Universe was dominated by matter in this state, making it a particularly important object of study [2]. QGP also offers an opportunity to test our understanding of QCD itself, particularly the perturbative and numerical techniques currently used in QCD analysis. The STAR detector at RHIC (Relativistic Heavy Ion Collider) was built primarily for the purpose of studying this exotic phase of matter.

QGP cannot be observed directly – the QGP created at RHIC exists for only 10^{-23} s before condensing into more familiar hadrons. Instead, its presence must be inferred indirectly from the behavior of these hadrons [3]. Despite this challenge, STAR has gathered conclusive proof of the formation of QGP at RHIC, observing a variety of phenomenon linked to quark deconfinement. One such phenomenon is the anisotropic expansion of the dense medium created in ion collisions, an effect which has been linked to the collective motion of constituent quarks during the QGP phase. This collective motion is known as elliptic flow, and is quantified by the parameter v_2 (discussed in Section 2.1). Elliptic flow is an important experimental tool, useful for a variety of experiments. It is used to test hydrodynamic models of quark motion, to investigate parity violation, and more [4] [5]. Elliptic flow has therefore been heavily investigated in Gold-Gold collisions.

It has been observed that, in these Au-Au collisions, v_2/ϵ scales with $1/S\ \mathrm{d}N_{ch}/\mathrm{d}\eta$, where ϵ is the eccentricity of the QGP region, S is its transverse area, and $\mathrm{d}N_{ch}/\mathrm{d}y$ is the multiplicity of charged particles per unit pseudo-rapidity. $\mathrm{d}N_{ch}/\mathrm{d}\eta$ may be more qualitatively thought to be the number of particles produced in the collision, and so $1/S\ \mathrm{d}N_{ch}/\mathrm{d}\eta$ is a proxy for the resulting parton density.

Certain experiments, particularly those two mentioned above, might benefit from larger v_2 than Au-Au collisions can provide [5]. In an attempt to increase v_2, RHIC has begun colliding Uranium ions. Uranium nuclei are larger and more oblong than Gold – Uranium is somewhat football shaped while Gold is roughly spherical. Due to its increased size, Uranium is expected to increase $1/S\ \mathrm{d}N_{ch}/\mathrm{d}\eta$ by over 13% [5], while Glauber Monte Carlo models predict a significant enhancement of v_2. In this paper, we present the first measurements of v_2 in U-U collisions, and compare these measurements to previous Au-Au results.

2 Theory

2.1 Elliptic Flow

A single heavy ion collision is diagrammed in Figure 1. As two ions pass by one another, the nucleons in their peripheries collide, leaving behind an ellipsoid QGP region with density $\sim 10^{12}$ kg/cm^3 [2]. Due to pressure gradients which form along its semi-minor axis, this medium expands predominately in the reaction plane (defined by the x and z axes). This effect, called elliptic flow, manifests itself as an anisotropy in the final distribution of detected hadrons.

Elliptic flow is driven by the initial geometry of the QGP region. This region is characterized by its eccentricity, defined by

$$\epsilon = \frac{\langle y^2 \rangle - \langle x^2 \rangle}{\langle y^2 \rangle + \langle x^2 \rangle}. \tag{1}$$

Also important is the region's area when projected onto the transverse plane (see Figure 2):

$$S = \pi \sqrt{\langle x^2 \rangle \langle y^2 \rangle}. \tag{2}$$

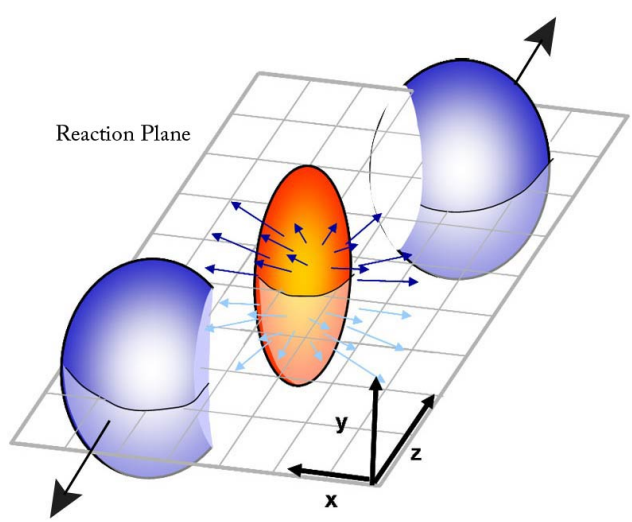

Figure 1: Heavy ion collision geometry. The beam direction defines the z-axis. As ions collide, they leave behind dense, ellipsoid-shaped QGP regions. The semi-major and semi-minor axes of this region define the y- and x-axis, respectively. The formation of pressure gradients drives this dense medium to expand primarily in the reaction plane, defined by the x and z axes. Figure adapted from: `http://www.interactions.org/sgtw/2006/1025/star_grid_more.html`.

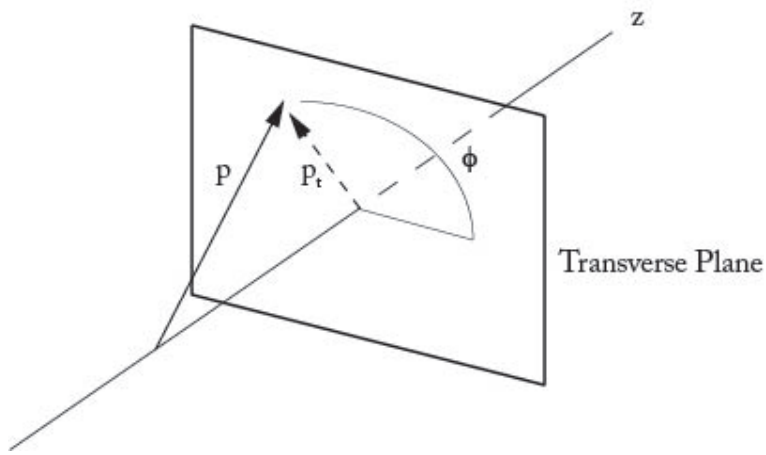

Figure 2: Transverse plane geometry. The transverse plane lies perpendicular to the beam direction. The azimuthal angle ϕ measures counter-clockwise around the z-axis. p is the magnitude of a particle's momentum, while p_t is its momentum projected onto the transverse plane.

These two parameters can be considered to determine the evolution of the QGP medium – higher ϵ yields increased elliptic flow, while increased area S indicates that more mass participates in the collision, resulting in greater particle production.

Elliptic flow may be quantified by reconstructing the angular distribution of particles created in ion collisions. The distribution of detected particles may be represented by [6]

$$E\frac{\mathrm{d}^3N}{\mathrm{d}p^3} = \frac{1}{2\pi}\frac{\mathrm{d}^2N}{p_t\mathrm{d}p_t\mathrm{d}y}\left[1 + 2\sum_{n=1}^{\infty} v_n \cos n\left(\phi - \Psi_{RP}\right)\right], \tag{3}$$

$$v_n = \langle \cos n\left(\phi - \Psi_{RP}\right)\rangle . \tag{4}$$

E is particle energy, p momentum, and N the number of detected particles. p_t is particle momentum in the transverse plane, while ϕ is the azimuthal angle at which the particle is detected; both are depicted in Figure 2. Ψ_{RP} is the azimuthal angle of the reaction plane, while y is rapidity, a quantity related to velocity in the z direction.

The Fourier expansion shown in (3) may be used to reconstruct the angular distribution (projected onto the transverse plane) of emitted particles. If Ψ_{RP} is known, the Fourier coefficients are easily calculated by averaging over all detected particles, following (4). Of particular importance is the second coefficient, v_2. Called the elliptic flow coefficient, this value is a direct measure of the strength of the anisotropic flow discussed above. Positive values indicate strong particle production along the semi-minor axis of the QGP region, while negative values correspond to particle flow along the semi-major axis.

2.2 Reaction Plane Estimation

Equations (3) and (4) require knowledge of the reaction plane angle. In any particular event, however, this is something we do not know *a priori*. The reaction plane must be reconstructed after-the-fact using trajectories of detected particles. This artificially reconstructed reaction plane is called the event plane. The event plane angle is given by [7]

$$\Psi_{EP} = \left(\tan^{-1}\frac{\sum_i w_i \sin n\phi_i}{\sum_i w_i \cos n\phi_i}\right)/n, \tag{5}$$

where w_i is a weighting factor. The event plane resolution, a measure of the accuracy of the above approximation, is [7]

$$\delta\Psi = \sqrt{\langle \cos n\,(\Psi_n^a - \Psi_n^b)\rangle}, \tag{6}$$

where Ψ_n^a and Ψ_n^b represent the event plane angle for two different subsets of data. Ψ_{EP} and its corresponding resolution may be calculated independently using any Fourier harmonic n. In our analysis, we chose $n = 2$, and calculated Ψ_n^a and Ψ_n^b using particles with positive and negative rapidities (positive and negative velocities), respectively. Replacing Ψ_{RP} with Ψ_{EP} in Equation (4) and dividing to account for finite event plane resolution finally gives

$$v_n = \frac{\langle \cos n\,(\phi - \Psi_{EP})\rangle}{\delta\Psi}. \tag{7}$$

The reaction/event plane orientations should be entirely random – the true distribution of Ψ_{EP} should therefore be isotropic between 0 and π. Due to imperfect detector sensitivities, however, the *detected* distribution is observed to be anisotropic. Calculated values of Ψ_{EP} must be further adjusted to account for this effect. A description of this process, known as event plane flattening, is given in Appendix A.

3 Data Collection and Procedure

Data was collected by the STAR detector at RHIC, during 2012 U-U collisions at $\sqrt{s_{NN}} = 193$ GeV and 2011 Au-Au collisions at $\sqrt{s_{NN}} = 200$ GeV. Only those particles with $|\eta| < 1$ and $0.15 < p_t < 2$ GeV/c, and whose paths originated within 2 cm of the collision site were accepted. η is known as pseudo-rapidity, an analogue to rapidity (speed) used when a particle's mass is not known. Collision events were sorted into three centrality bins based on their charged particle multiplicities. Collisions with higher multiplicities likely resulted from more head-on, or more *central* ion collisions. Lower multiplicities correspond to less central, or more edge-on collisions. Event planes were then flattened independently for each centrality bin.

Using Equation (7), we calculated v_2 as a function of multiplicity $\mathrm{d}N/\mathrm{d}\eta$. Multiplicity was determined in several different ways. It was typically calculated by counting the number of distinct charged particles with $|\eta| < 0.5$ detected in the STAR Time Projection Chamber (TPC), an instrument which recreates charged particles' paths through the STAR detector. Multiplicity may also be calculated by counting the number of detections in the Time-of-Flight instrument (TOF), which surrounds the beam azimuthally. The eccentricity ϵ and transverse area S of the QGP region cannot be experimentally measured. Instead they were calculated with Glauber simulations as a function of detected multiplicity, and matched to observed data.

4 Results and Analysis

Shown in Figure 3 is the measured v_2 as a function of charged particle multiplicity for both Au-Au and U-U collisions. It may be seen that Uranium collisions result in higher particle multiplicities as well as larger values of v_2, as predicted. Particle multiplicity was determined using TPC tracks. Multiplicity is labelled as "uncorrected" since we have not yet accounted for the variability of detector efficiency across different multiplicity values. This correction will result in increased values of $\mathrm{d}N/\mathrm{d}\eta$, but will not affect v_2 – it will therefore not affect the qualitative nature of the results presented here.

Figure 4 shows v_2/ϵ vs. $1/S\ \mathrm{d}N_{ch}/\mathrm{d}\eta$ for Au-Au and U-U. For Gold, v_2/ϵ increases monotonically. Elliptic flow is a response to the initial spatial anisotropy of the QGP region, quantified by eccentricity ϵ. Plotting v_2/ϵ, therefore, should remove the geometry dependence and move all points onto a universal curve, traced by the Au-Au data points in Figure 4 [1]. Results from other ion collisions, such as Copper-Copper and Lead-Lead, also conform to this curve across a range of energies. Uranium, however, does not seem to obey this scaling. Although it traces the Au-Au curve nearly perfectly until $1/S\ \mathrm{d}N_{ch}/\mathrm{d}\eta \approx 20$, the U-U data drops significantly past this point.

This was not predicted in Glauber simulations. In order to verify this result, the U-U analysis was repeated using both TPC and TOF multiplicities, as well as TOF matching, a process which requires

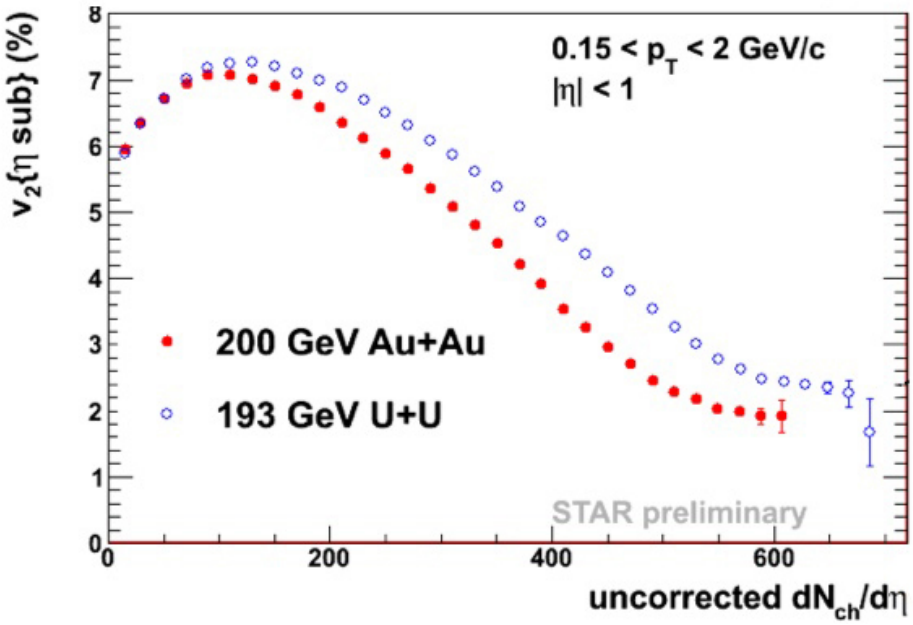

Figure 3: v_2 vs. charged particle multiplicity for Au-Au and U-U collisions. $\mathrm{d}N/\mathrm{d}\eta$ is determined by the number of reconstructed TPC tracks. Multiplicities have not been corrected to account for detector inefficiencies. As predicted, U-U collisions result in increased multiplicities and v_2.

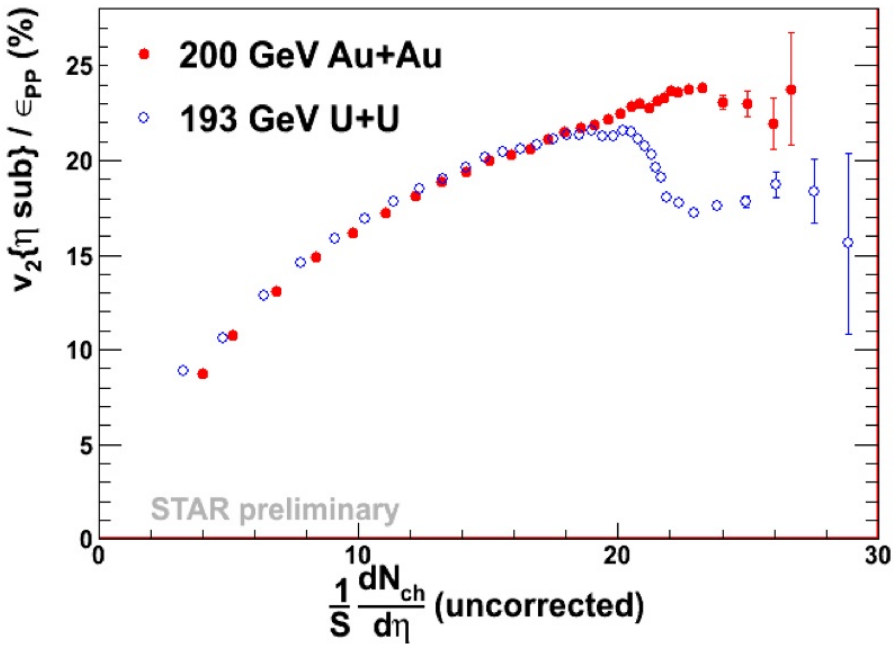

Figure 4: v_2/ϵ vs. $1/S\ \mathrm{d}N/\mathrm{d}\eta$ for Au-Au and U-U collisions. In dividing v_2 by ϵ, the geometry dependence seen in Figure 3. The Au-Au data increases monotonically, tracing a universal curve also followed by Cu-Cu and Pb-Pb collisions. Uranium, however, does not conform to this curve. This is likely due to overestimation of ϵ at high multiplicities.

accepted particles to contribute signals to *both* the TOF and TPC detectors. TOF matching eliminates potential pile-up (accidental detection of particles produced in other collisions) and spurious signals. Analysis was also repeated using a central cut on U-U data, which isolates only the most central ion collisions. These approaches all yielded results consistent with the trends seen in Figures 3 and 4.

One possible conclusion is that the universal curve traced by Au-Au in Figure 4 is not, in fact, universal. However, since a variety of other systems agree well with the Au-Au curve, this conclusion is likely incorrect. More likely is that the present understanding of particle production in ion collisions is incomplete. In this case, the values of ϵ and S calculated in Glauber simulations of U-U collisions may be incorrectly matched to particle multiplicity. Overestimation of ϵ in very central collisions, for instance, might be responsible for the deviation of U-U at high multiplicities in Figure 4.

The Glauber models used to generate ϵ and S should therefore be revisited. Assuming that the U-U and Au-Au curves in Figure 4 should coincide, in the future the Glauber models should be adjusted with the goal of forcing the high multiplicity U-U data points back onto the universal curve. This effectively provides a metric by which various Glauber models can be tested – ideally the correct model is the one which best matches U-U data to the Au-Au curve.

5 Conclusion

In order to attain increased values of v_2, RHIC has begun colliding Uranium ions at $\sqrt{s_{NN}} = 193$ GeV. Glauber simulations predicted Uranium collisions to result in increased v_2 as well as increased particle multiplicities, a prediction confirmed here. v_2/ϵ, however, does not increase monotonically with $1/S\ \mathrm{d}N_{ch}/\mathrm{d}\eta$ in U-U collisions – it deviates significantly from the supposedly universal curve set by Gold data, a result not predicted by current theory. It is therefore likely that Glauber models used to calculate ϵ and S in Uranium collisions are incomplete, resulting in the deviation seen at high multiplicities. These models should therefore be revisited, in an effort to remove the potentially artificial deviation of v_2/ϵ.

Acknowledgements

I would like to thank Dr. Huan Huang and Dr. Gang Wang at UCLA for their all of their help and support this summer. I would like to thank the NSF for funding my summer research, and Françoise Queval for her wonderful job organizing the REU program. Finally, I would like to thank my fellow REU students for making this summer so much fun.

References

[1] E. Shuryak. What rhic experiments and theory tell us about properties of quark-gluon plasma? *Nuclear Physics A*, 750, 2005.

[2] J. Letessier and J. Rafelski. *Hadrons and Quark-Gluon Plasma.* Cambridge University Press, 2002.

[3] K. Yagi, T. Hatsuda, and Y. Miake. *Quark-Gluon Plasma.* Cambridge University Press, 2005.

[4] Y. Burnier, D. Kharzeev, J. Liao, and H. Yee. Chiral magnetic wave at finite baryon density and the electric quadrupole moment of quark-gluon plasma in heavy ion collisions. *Phys. Rev. Lett.*, 107, 2011.

[5] C. Nepali, G. Fai, and D. Keane. Advantage of u+u over au+au collisions at constant beam energy. *Phys. Rev. C*, 73, 2006.

[6] B. Biritz. *Electron-hadron azimuthal correlations in Au+Au collisions at* $\sqrt{s_{NN}} = 200$ *Gev.* PhD thesis, University of California, Los Angeles, 2010.

[7] A. Poskanzer and S. Voloshin. Methods for analyzing anisotropic flow in relativistic nuclear collisions. *Phys. Rev. C*, 58, 1998.

[8] G. Wang. *Correlations relative to the reaction plane at the relativistic heavy ion collider based on transverse deflection of spectator neutrons.* PhD thesis, Kent State University, 2006.

A Flattening the Event Plane Distribution

The reaction plane for each ion collision should be randomly oriented, and so the event plane distribution for a set of collisions should be flat. However, due to limitations in detector hardware and sensitivity, not all angles can be detected with the same efficiency, and so we observe an anisotropic distribution. A raw Ψ_{EP} distribution for a large number of events is shown in Figure 5a.

Following [8], the event plane distribution may be written as a Fourier series:

$$\frac{\mathrm{d}N}{\mathrm{d}\psi} = \frac{a_0}{2} + \sum_n \left(a_n \cos n\psi + b_n \sin n\psi\right). \tag{8}$$

A new angle $\psi\prime$ may be defined by

$$\begin{aligned} \psi\prime &= \psi + \Delta\psi \\ &= \psi + \sum_n \left(A_n \cos n\psi + B_n \sin n\psi\right), \end{aligned} \tag{9}$$

where in the last step $\Delta\psi$ has also been expressed as a Fourier series, with coefficients A_n and B_n. Requiring that event plane angles be uniformly distributed over $\psi\prime$,

$$\begin{aligned} \frac{\mathrm{d}N}{\mathrm{d}\psi\prime} &= \frac{N}{2\pi} \\ &= \frac{a_0}{2}, \end{aligned} \tag{10}$$

since the coefficient a_0 represents the average value of $\mathrm{d}N/\mathrm{d}\psi$. Using the chain rule, $\mathrm{d}N/\mathrm{d}\psi$ may now be rewritten as

$$\begin{aligned} \frac{\mathrm{d}N}{\mathrm{d}\psi} &= \frac{\mathrm{d}N}{\mathrm{d}\psi\prime}\frac{\mathrm{d}\psi\prime}{\mathrm{d}\psi} \\ &= \frac{a_0}{2}\left(1 + \sum_n \left(-nA_n \sin n\psi + nB_n \cos n\psi\right)\right), \end{aligned} \tag{11}$$

differentiating (9) by ψ in the final step. Comparing (8) and (11), the coefficients A_n and B_n are seen to be

$$A_n = -\frac{2}{n}\frac{b_n}{a_0} = -\frac{2}{n}\left\langle \sin n\psi \right\rangle \tag{12}$$

$$B_n = -\frac{2}{n}\frac{a_n}{a_0} = -\frac{2}{n}\left\langle \cos n\psi \right\rangle. \tag{13}$$

Substituting (12) and (13) into (9), the corrected event plane angle is given by

$$\psi\prime = \psi + \sum_n \frac{2}{n}\left(-\left\langle \sin n\psi \right\rangle \cos n\psi + \left\langle \cos n\psi \right\rangle \sin n\psi\right). \tag{14}$$

This approach effectively shifts each event plane angle until the final distribution is isotropic [7]. Figure 5b shows the event plane distribution from Figure 5a, after being flattened with (14).

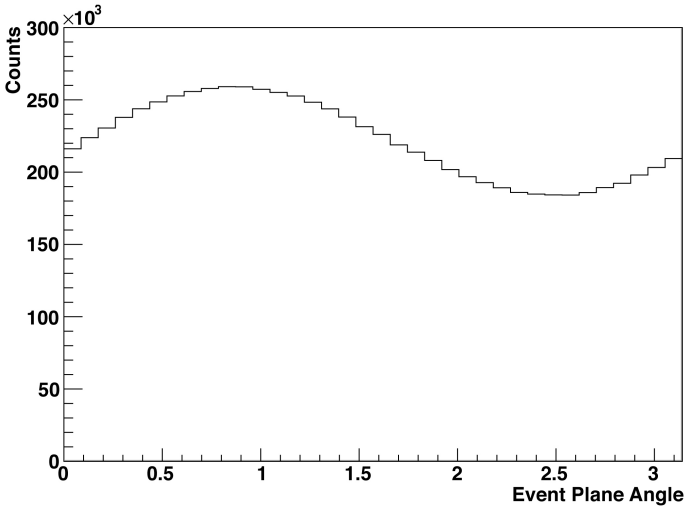

(a) Raw Distribution

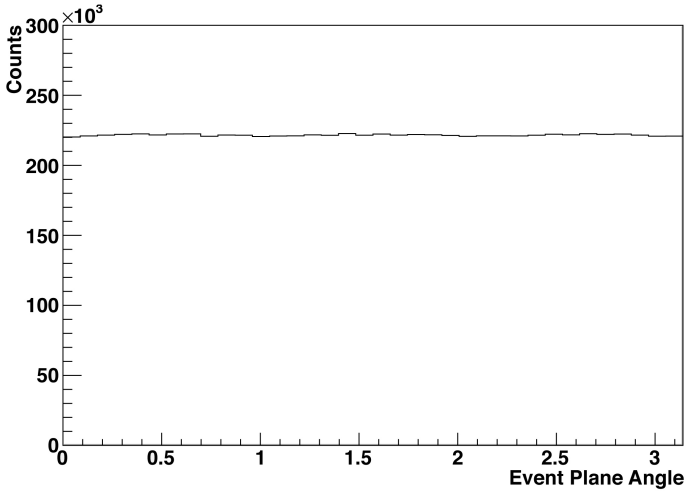

(b) Flattened Distribution

Figure 5: (a) Raw event plane angle distribution. Due to detector inefficiencies, the initial recorded distribution is anisotropic, despite the underlying isotropic distribution. (b) The same distribution, flattened using Equation (14).